

Spectrum of coherent backscattering of light by two atoms

Vyacheslav Shatokhin*

B. I. Stepanov Institute of Physics, National Academy of Sciences, 220072 Minsk, Belarus

(Dated: July 27, 2018)

We study theoretically inelastic spectrum of coherent backscattering of laser light by two atoms. For an intense laser field, there are frequency domains of not only constructive but also destructive (self-)interference of the inelastic photons. We interpret the emergent spectral features using the dressed states and considering coherent backscattering as a kind of the pump-probe experiment.

I. INTRODUCTION

Remarkable progress in laser cooling and trapping of atomic gases [1] that led to a realization of Bose-Einstein condensate [2] made it also possible an exploration of various mesoscopic transport and localization phenomena [3] using cold atomic gases. In particular, possessing large (compared to their geometric size) and easily manipulated scattering cross-section, atoms turned out to be suitable for studying light transport in the weak and, prospectively, strong localization regimes. Recently, coherent backscattering (CBS) of resonant laser light (an analog of weak localization of electrons in disordered conductors) has been observed with cold, trapped atomic clouds [4, 5]. Since then, CBS of light by cold atoms has become an area of intense theoretical and experimental research (for a recent review, see [6]).

Coherent backscattering is an enhancement of the average intensity of light reflected off a dilute, disordered medium in the backscattering direction. The underlying physical reason for the emergence of CBS is the constructive interference between the counterpropagating (labelled “direct” and “reversed”) multiple scattering amplitudes. When a scattering medium consists of individual atoms, several mechanisms affecting phase coherence between the interfering amplitudes should be considered. These are (i) Raman scattering on degen-

*Electronic address: v.shatokhin@dragon.bas-net.by

erate atomic transitions; (ii) inelastic scattering; (iii) mechanical motion of atoms.

As regards the atomic degeneracy mediating Raman processes accompanied by photon polarization flips, its dephasing role is nowadays very well understood, with quantitative accordance between theory [7, 8, 9] and experiment [5, 10], for ensembles of Rb atoms.

The next dephasing mechanism, the inelastic photon scattering induced by atomic saturation s , has been studied in less detail. Recent experiment with cold Sr atoms demonstrated a rapid decrease of CBS enhancement factor α versus saturation at moderate $s \leq 1$ [11]. It was shown, within a scattering theory approach applied to two atoms in the regime of weakly nonlinear scattering [12], that a decrease of CBS enhancement factor occurs due to the partial distinguishability of the interfering amplitudes. In the general case of many atoms, three different amplitudes interfere constructively in the weakly nonlinear regime, so that α may exceed the linear barrier 2 [13].

In this contribution, we will also be concerned with the impact of saturation on CBS, though for arbitrary laser field intensities. But prior to proceed with a presentation of this work, let us make a brief note on the effect of thermal motion of atoms at temperatures on the order $100 \mu\text{K}$ typical for CBS experiments.

Mechanical motion spoils phase coherence between the direct and reversed amplitudes [14] if spread v of the atomic velocities violates the resonance condition $kv \ll 2\gamma$ [15], where k is the wave number and 2γ is the natural linewidth of the excited atomic state. In the regime of weak laser intensities, this inequality is usually satisfied, and the picture of motionless atoms works very well so long as the CBS intensity is concerned [7]. However, already in the elastic scattering regime, the photon recoil and Doppler effects do modify the CBS spectrum [16]. It is even more so in the inelastic scattering regime, when the atoms from the cloud are rapidly accelerated out of resonance by a powerful laser field. Nonetheless, we will ignore this acceleration and assume that the atoms are fixed in space. Thus, we focus here on the laser field coupling exclusively to the atomic internal degrees of freedom, in order to highlight the fundamental interference effect under the influence of the nonlinear scattering. Explanation of this influence for atoms at rest is basic to its understanding for atoms in motion.

More specifically, we will study spectrum of CBS by two atoms in the helicity preserving polarization channel. This topic is above all motivated by our previous work [17, 18], where we established existence of the residual CBS contrast in the deep saturation regime,

due to the constructive (self-)interference of inelastically scattered photons. However, this constructive interference is a net effect of all inelastic photons. The question that naturally arises, of what the character of interference is at a given frequency, can only be answered after looking at the CBS spectrum. In this work we answer this question for the particular case of exact resonance. We demonstrate that, in the saturation regime, there are frequency domains where the interferential contribution exhibits not only constructive but also destructive interference, and employ the pump-probe analysis and the dressed states representation to identify the scattering processes that are responsible for the emergent spectral features. Our results agree with those derived within the Langevin equation approach [19].

The paper is organized as follows: We start with a brief presentation of our model and the master equation approach that we are using. In Sect. III we present results for the stationary CBS intensity and enhancement factor, and thereafter for CBS spectrum. In the last Section, we conclude our work.

II. MASTER EQUATION APPROACH TO CBS OF LIGHT BY TWO ATOMS

A. Model and the main quantity of interest

Details of our approach are given in Ref. [18]. Here, we will only present its brief outline. We consider a model quantum system consisting of 2 identical, motionless atoms located at positions \mathbf{r}_1 and \mathbf{r}_2 , with the distance $r_{12} = |\mathbf{r}_1 - \mathbf{r}_2|$ being much greater than the optical wavelength. The atoms are embedded in the electromagnetic bath of quantized harmonic oscillators and subjected to an external laser field of arbitrary intensity [See Fig. 1(a)]. Coupling to the bath gives rise to the spontaneous emission from the excited state and to the far-field dipole-dipole interaction responsible for exchange of photons, whereas coupling to the laser field gives rise to the Rabi oscillations of populations and coherences in the laser-driven transitions of both atoms. Although this approach can, of course, be formulated for atoms with arbitrary internal structure, we choose the ground states of the atoms to be nondegenerate, while the excited state 3-fold degenerate [see Fig. 1(b)]. An important parameter describing the effect of a laser field on atoms is the so-called saturation parameter $s = \Omega^2/2(\gamma^2 + \delta^2)$, where Ω is the Rabi frequency and $\delta = \omega_L - \omega_0$ is the detuning of the laser field with respect to atomic resonance. As already mentioned, here we will be interested in

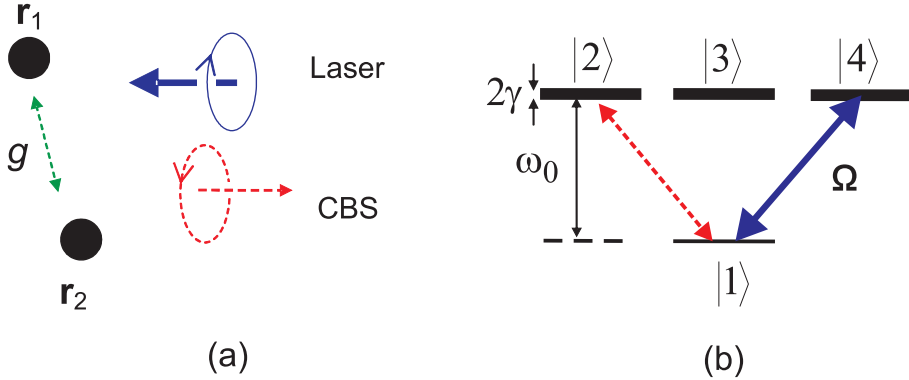


FIG. 1: Model of CBS with two atoms. (a) atoms (black dots) are driven by laser light with right circular polarization, while CBS is observed in the helicity preserving channel, that is, with flipped polarization. Photons in this channel appear as a result of double scattering. g is the strength of the far-field dipole-dipole coupling responsible for exchange of photons; (b) internal atomic structure corresponding to a $J_g = 0 \rightarrow J_e = 1$ dipole transition. ω_0 is the transition frequency, 2γ is the radiative linewidth, Ω is the Rabi frequency. Sublevels $|1\rangle$ and $|3\rangle$ have magnetic quantum number $m = 0$. Sublevels $|2\rangle$ and $|4\rangle$ correspond to $m = -1$ and $m = 1$, respectively. Thick solid arrow shows laser field driving $|1\rangle \leftrightarrow |4\rangle$ transition, while dashed arrow shows CBS field originating from $|1\rangle \leftrightarrow |2\rangle$ transition.

how the spectrum of CBS behaves as a function of s at $\delta = 0$. In this case, all results can be deduced in an analytic form.

Raman processes which can strongly affect CBS do not take place on the $J_g = 0 \rightarrow J_e = 1$ transition under consideration. Furthermore, incoherent single scattering contribution can be filtered out by looking at CBS, e.g., in the helicity preserving ($h \parallel h$) polarization channel. Precisely this channel was probed in a recent experiment with cold Sr atoms [11]. We consider the particular case of the laser light with the right circular polarization, that is, $\epsilon_L = \hat{\mathbf{e}}_{+1}$, in the helicity basis notation. Hence, CBS with preserved helicity corresponds to the flipped polarization $\epsilon = \hat{\mathbf{e}}_{-1}$ as shown on Fig. 1.

Spectrum of CBS to be addressed in this paper is derived from the average value of the first-order field temporal correlation function [20]:

$$G^{(1)}(\mathbf{r}, t; \mathbf{r}, t') = \langle \text{Tr} \{ \rho [\epsilon \cdot \mathbf{E}^{(-)}(\mathbf{r}, t)][\epsilon^* \cdot \mathbf{E}^{(+)}(\mathbf{r}, t')] \} \rangle_{\text{conf}}, \quad (1)$$

where ρ is the initial density operator of the atom-field system, $\mathbf{E}^{(-/+)}(\mathbf{r}, t)$ is the negative/positive frequency component of the electric field operator of the scattered field, and

$\langle \dots \rangle_{\text{conf}}$ denotes configuration averaging. The components of the scattered field are the retarded fields radiated by the atomic dipoles,

$$\mathbf{E}^{(+)}(\mathbf{r}, t) = \frac{\omega_0^2}{4\pi\epsilon_0 c^2 r} \sum_{\alpha=1}^2 \mathbf{D}_\alpha(t_\alpha) e^{-i\mathbf{k}\cdot\mathbf{r}_\alpha}, \quad (2)$$

where ϵ_0 is the permittivity of the vacuum, $\mathbf{D}_\alpha = -\hat{\mathbf{e}}_{-1}\sigma_{12}^\alpha + \hat{\mathbf{e}}_0\sigma_{13}^\alpha - \hat{\mathbf{e}}_{+1}\sigma_{14}^\alpha$, with $\sigma_{kl}^\alpha \equiv |k\rangle_\alpha \langle l|_\alpha$, is the dipole lowering operator, and $t_\alpha = t - |\mathbf{r} - \mathbf{r}_\alpha|/c$. In writing Eq. (2), we have assumed that $r_{12} \ll r$, that is, the field is detected in the radiation zone at the distance much larger than the interatomic distance. In the following, we will for brevity omit the r -dependent prefactor of Eq. (2) and, consistently, of the temporal correlation functions.

Inserting Eq. (2) into Eq. (1) we obtain, in the steady state limit $t \rightarrow \infty$,

$$G_{\text{ss}}^{(1)}(\tau) = \sum_{\alpha, \beta=1}^2 \langle \langle \sigma_{21}^\alpha \sigma_{12}^\beta(\tau) \rangle_{\text{ss}} \rangle_{\text{conf}} e^{i\mathbf{k}\cdot\mathbf{r}_{\alpha\beta}}, \quad (3)$$

where “ss” stands for *steady state*, $\tau = t' - t \geq 0$, the inner angular brackets indicate quantum mechanical expectation value [see Eq. (1)], and $\mathbf{r}_{\alpha\beta} \equiv \mathbf{r}_\alpha - \mathbf{r}_\beta$.

Spectrum can be obtained via Laplace transform of (3) [21]:

$$S(\nu) = \frac{1}{\pi} \lim_{\Gamma \rightarrow 0} \text{Re} \{ \tilde{G}_{\text{ss}}^{(1)}(z) \}, \quad (4)$$

where $\tilde{G}_{\text{ss}}^{(1)}(z) = \int_0^\infty d\tau \exp(-z\tau) G_{\text{ss}}^{(1)}(\tau)$, $z = \Gamma - i\nu$ with $\Gamma \geq 0$ and $\nu = \omega - \omega_L$. Note that the spectrum is defined with respect to the laser frequency which means that the atomic correlation functions must be evaluated in the frame rotating at ω_L .

Let us conclude this subsection with a remark on the configuration averaging procedure. This procedure is necessary because the two-atom correlation functions may sensitively depend on the interatomic distance and orientation of the vector \mathbf{r}_{12} with respect to \mathbf{k}_L , exhibiting rapid oscillations around the backscattering direction. These oscillations have the same nature as a speckle pattern scattered off a disordered medium. After many realizations of the disorder, all peaks except the one, corresponding to CBS, disappear. A simple and sufficient way to mimic disorder in a two-atom system is to assume an isotropic distribution of the radius-vector connecting the atoms and a uniform distribution of interatomic distances around the average distance ℓ equal to the scattering mean free path.

B. Master equation

To find the atomic correlation functions appearing in the right hand side of Eq. (3) we have adapted [17, 18] a theoretical approach initiated by Lehmberg in 1970 [22]. Within this approach, dynamics of the dipole operators' expectation values as well as dipole-dipole correlators is governed by the master equation

$$\langle \dot{Q} \rangle = \sum_{\alpha=1}^2 \langle \mathcal{L}_\alpha Q \rangle + \sum_{\alpha \neq \beta=1}^2 \langle \mathcal{L}_{\alpha\beta} Q \rangle, \quad (5)$$

where the Liouvillians \mathcal{L}_α and $\mathcal{L}_{\alpha\beta}$ generate the time evolution of an arbitrary atomic operator Q , for independent and interacting atoms, respectively. Explicitly,

$$\begin{aligned} \mathcal{L}_\alpha Q &= -i\delta[\mathbf{D}_\alpha^\dagger \cdot \mathbf{D}_\alpha, Q] - \frac{i}{2}[\Omega_\alpha(\mathbf{D}_\alpha^\dagger \cdot \boldsymbol{\varepsilon}_L) + \Omega_\alpha^*(\mathbf{D}_\alpha \cdot \boldsymbol{\varepsilon}_L^*), Q] \\ &\quad + \gamma (\mathbf{D}_\alpha^\dagger \cdot [Q, \mathbf{D}_\alpha] + [\mathbf{D}_\alpha^\dagger, Q] \cdot \mathbf{D}_\alpha), \end{aligned} \quad (6)$$

$$\mathcal{L}_{\alpha\beta} Q = \mathbf{D}_\alpha^\dagger \cdot \overleftrightarrow{\mathbf{T}}(g, \hat{\mathbf{n}}) \cdot [Q, \mathbf{D}_\beta] + [\mathbf{D}_\beta^\dagger, Q] \cdot \overleftrightarrow{\mathbf{T}}^*(g, \hat{\mathbf{n}}) \cdot \mathbf{D}_\alpha, \quad (7)$$

where $\Omega_\alpha = \Omega e^{i\mathbf{k}_L \cdot \mathbf{r}_\alpha}$. The radiative dipole-dipole interaction due to exchange of photons between the atoms is described by the tensor $\overleftrightarrow{\mathbf{T}}(g, \hat{\mathbf{n}}) = \gamma g \overleftrightarrow{\Delta}$, with $\overleftrightarrow{\Delta} = \overleftrightarrow{1} - \hat{\mathbf{n}}\hat{\mathbf{n}}$ being the projector on the transverse plane defined by the unit vector $\hat{\mathbf{n}}$ along the connecting line between the atoms α and β . This interaction has a certain strength depending on the distance between the atoms, via

$$g = \frac{3i}{2k_0 r_{\alpha\beta}} e^{ik_0 r_{\alpha\beta}}, \quad (8)$$

with $k_0 = \omega_0/c$, and on the life time of the excited atomic levels, through γ . The coupling constant $|g| \ll 1$ is small in the far-field ($k_0 r_{\alpha\beta} \gg 1$), where near-field interaction terms of order $(k_0 r_{\alpha\beta})^{-2}$ and $(k_0 r_{\alpha\beta})^{-3}$ can be neglected.

Of course, an arbitrary operator Q inserted into Eq. (5) does not result in a closed differential equation. Our system consisting of two 4-level atoms leads to $255 = 4^2 \cdot 4^2 - 1$ linear coupled equations of motion for the one-time averages. We solve them perturbatively up to g^2 , to account for the lowest order (double-)scattering process giving rise to a nontrivial interferential contribution. To help the reader keeping this in mind we will supply symbols denoting double scattering intensities and spectra with the subscript “2”.

Note that Eq. (5) describes evolution of the expectation values (one-time correlation functions), whereas $G_{ss}^{(1)}(\tau)$ is the *two*-time correlation function. By virtue of the quantum regression theorem [21], the latter satisfy Eq. (5) also, but their initial conditions are extracted from the stationary solution of (5). In particular, the double scattering counterpart of $G_{ss}^{(1)}(0)$ is nothing but the stationary average backscattered light intensity which will be referred to as I_2^{tot} . There is an obvious relation between I_2^{tot} and $S_2(\nu)$:

$$I_2^{\text{tot}} = \int_{-\infty}^{\infty} d\nu S_2(\nu). \quad (9)$$

The expression for I_2^{tot} can be obtained independently from (9). We will use this independent derivation as an implicit verification of our results for CBS spectra.

The total CBS intensity at the backscattering direction can be decomposed in the sum of two terms

$$I_2^{\text{tot}} = L_2^{\text{tot}} + C_2^{\text{tot}}, \quad (10)$$

where $C_2^{\text{tot}} \equiv C_2^{\text{tot}}(\theta = 0)$ (i.e., $\mathbf{k} = -\mathbf{k}_L$), and

$$C_2^{\text{tot}}(\theta) = 2 \operatorname{Re} \langle \langle \sigma_{21}^1 \sigma_{12}^2 \rangle_{\text{ss}}^{[2]} e^{i\mathbf{k} \cdot \mathbf{r}_{12}} \rangle_{\text{conf}}, \quad (11)$$

$$L_2^{\text{tot}} = \langle \langle \sigma_{22}^1 \rangle_{\text{ss}}^{[2]} + \langle \sigma_{22}^2 \rangle_{\text{ss}}^{[2]} \rangle_{\text{conf}}, \quad (12)$$

are the so called crossed and ladder terms, respectively. Using these terms we can derive a standard measure of phase coherence between the counterpropagating amplitudes in CBS – the enhancement factor

$$\alpha = 1 + \frac{C_2^{\text{tot}}}{L_2^{\text{tot}}}, \quad (13)$$

which for perfect two-wave interference is equal to 2.

Generally, the total backscattered light intensity has the elastic and inelastic counterparts,

$$I_2^{\text{tot}} = I_2^{\text{el}} + I_2^{\text{inel}}. \quad (14)$$

The elastic counterpart is given by the product of the expectation values of the atomic dipoles,

$$I_2^{\text{el}} = \sum_{\alpha, \beta=1}^2 \langle \langle \sigma_{21}^{\alpha} \rangle_{\text{ss}} \langle \sigma_{12}^{\beta} \rangle_{\text{ss}} e^{-i\mathbf{k}_L \cdot \mathbf{r}_{\alpha\beta}} \rangle_{\text{conf}}, \quad (15)$$

wherfrom for $\alpha = \beta$ we obtain the elastic ladder term L_2^{el} and for $\alpha \neq \beta$ the elastic crossed term C_2^{el} . Given I_2^{tot} and I_2^{el} we can find the fluctuating part of the dipole correlation functions defining I_2^{inel} .

III. RESULTS

A. CBS intensity and enhancement factor

The interferential contribution and the incoherent sum, Eqs. (11) and (12), yield results [18]

$$2 \operatorname{Re} \{ \langle \sigma_{21}^1 \sigma_{12}^2 \rangle_{\text{ss}}^{[2]} e^{i\mathbf{k} \cdot \mathbf{r}_{12}} \} = |g|^2 |\overleftrightarrow{\Delta}_{+1,+1}|^2 \frac{R_1(s)}{(4+s)P(s)} \times \cos\{(\mathbf{k} + \mathbf{k}_L) \cdot \mathbf{r}_{12}\}, \quad (16)$$

$$\langle \sigma_{22}^1 \rangle_{\text{ss}}^{[2]} + \langle \sigma_{22}^2 \rangle_{\text{ss}}^{[2]} = |g|^2 |\overleftrightarrow{\Delta}_{+1,+1}|^2 \frac{R_2(s)}{P(s)}. \quad (17)$$

$R_1(s)$, $R_2(s)$, and $P(s)$ are polynomial expressions in the on-resonance saturation parameter $s = \Omega^2/2\gamma^2$,

$$R_1(s) = \frac{2}{9} (6912s + 3168s^2 + 264s^3 + 20s^4 + s^5), \quad (18a)$$

$$R_2(s) = \frac{1}{3} (1152s + 528s^2 + 132s^3 + 7s^4), \quad (18b)$$

$$P(s) = (1+s)^2(12+s)(32+20s+s^2), \quad (18c)$$

and $\overleftrightarrow{\Delta}_{+1,+1} = \hat{\mathbf{e}}_{+1} \cdot \overleftrightarrow{\Delta} \cdot \hat{\mathbf{e}}_{+1}$.

The configuration average of (16) and (17) leads to the final result

$$C_2^{\text{tot}}(\theta) \simeq \frac{|\tilde{g}|^2 R_1(s)}{(4+s)P(s)} \left(\frac{2}{15} - \frac{(k\ell\theta)^2}{35} \right), \quad (19)$$

$$L_2^{\text{tot}} = \frac{2|\tilde{g}|^2 R_2(s)}{15P(s)}, \quad (20)$$

with $\tilde{g} = g|_{r_{\alpha\beta}=\ell}$. The scattering angle $\theta = 2 \arcsin\{|\mathbf{k} + \mathbf{k}_L|/2k_L\} \ll 1$ with respect to the backscattering direction was assumed to be sufficiently small herein.

The enhancement factor $\alpha(s)$, Eq. (13), deduced from Eqs. (19) and (20) reads

$$\alpha(s) = 1 + \frac{R_1(s)}{(4+s)R_2(s)}, \quad (21)$$

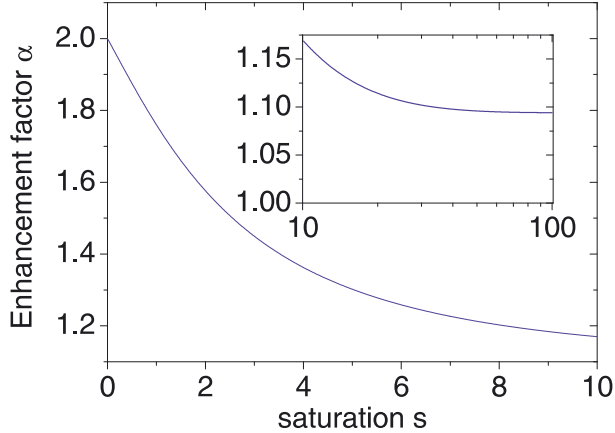


FIG. 2: Enhancement factor in the $h \parallel h$ channel versus saturation s . Decrease of α at small s is described by the linear function $2 - s/4$ in accordance with [12]. Inset describes α in the deep saturation regime. Enhancement tends to the limit $\alpha_\infty = 23/21$ [18] indicating constructive self-interference of inelastic photons.

and $\alpha(0) = 2.0$ in the weak field limit, as expected. The dependence of α on the saturation parameter is shown on Fig. 2. For small s , enhancement linearly decreases as $2 - s/4$, in full agreement with the diagrammatic theoretical result [12] and in qualitative agreement with the result of Sr experiment [11]. When s increases further, α monotonically drops to an asymptotic value $\lim_{s \rightarrow \infty} \alpha(s) = \alpha_\infty = 23/21$ [18] which is strictly larger than unity, implying a nonvanishing residual CBS contrast in the limit of large injected intensities. We will next show that this residual enhancement is due to inelastic photons only. Indeed, we obtained the following result for the elastic ladder and crossed terms

$$L_2^{\text{el}} = C_2^{\text{el}} = \frac{2|\tilde{g}|^2}{15} \frac{s}{(1+s)^4}. \quad (22)$$

As seen from Eq. (22), the elastic component shows perfect contrast for all s . In particular, it is this component that results in enhancement $\alpha = 2$ for very small $s \rightarrow 0$. However, in the deep saturation regime, this component decreases as s^{-3} , while the counterparts of the total intensity, Eqs. (19), (20), as s^{-1} . Herefrom follows our conclusion about the origin of the residual enhancement in the deep saturation regime. Explicitly, the inelastic crossed and ladder terms obtained by elementary subtraction of Eq. (22) from Eqs. (19) and (20)

read

$$C_2^{\text{inel}} = \frac{2|\tilde{g}|^2}{15} \frac{20736s^2 + 23424s^3 + 7108s^4 + 601s^5 + 44s^6 + 2s^7}{9(1+s)^2(4+s)P(s)}, \quad (23)$$

$$L_2^{\text{inel}} = \frac{2|\tilde{g}|^2}{15} \frac{2016s^2 + 2244s^3 + 796s^4 + 146s^5 + 7s^6}{3(1+s)^2P(s)}. \quad (24)$$

It is easy to verify that $\lim_{s \rightarrow \infty} C_2^{\text{inel}}/L_2^{\text{inel}} = 2/21 = \alpha_\infty - 1$.

B. CBS spectrum

Double scattering spectrum of CBS has the elastic and inelastic components. The elastic spectrum at the backscattering direction reads

$$\tilde{I}_2^{\text{el}}(\nu) = I_2^{\text{el}}\delta(\nu), \quad (25)$$

where $\delta(\nu)$ is the Dirac's delta-function, and $I_2^{\text{el}} = L_2^{\text{el}} + C_2^{\text{el}}$, with the ladder and crossed contributions defined in Eq. (22).

Inelastic spectra of the normalized ladder and crossed terms, for increasing values of Rabi frequencies, are shown on Fig. 3. Normalization is chosen such that integrals of $\tilde{L}_2^{\text{inel}}(\nu)/L_2^{\text{inel}}$ and $\tilde{C}_2^{\text{inel}}(\nu)/L_2^{\text{inel}}$ over ν yield unity and $C_2^{\text{inel}}/L_2^{\text{inel}}$, respectively. In the deep saturation regime, the value of the latter integral tends to the asymptotic value of the interference contrast of CBS, $\alpha_\infty - 1$.

In describing the CBS spectrum, it is natural to use two parameters Ω and γ defining positions and linewidths of spectral peaks rather than a single saturation parameter s . We will utilize s only to check consistency of our expressions for spectra with the results for the inelastic intensity and the enhancement factor.

As seen from Fig. 3, inelastic spectra are symmetric with respect to the laser frequency, for all Ω . For a small value of the Rabi frequency $\Omega = 0.1\gamma$ [Fig. 3(a)], spectra of both the ladder and crossed contributions have single peaks at $\nu = 0$. Interferential contribution $\tilde{C}_2^{\text{inel}}(\nu)$ is positive, though $\tilde{C}_2^{\text{inel}}(\nu) \leq \tilde{L}_2^{\text{inel}}(\nu)$ indicating that interference is not perfect in this weakly inelastic regime. We can derive analytical expressions for the curves of Fig. 3(a) by leaving the leading-order contribution to inelastic scattering $\sim (\Omega/\gamma)^4$, corresponding to two-photon processes, and neglecting the higher-order terms.

The ladder and crossed terms yield the compact expressions (henceforth, we will omit

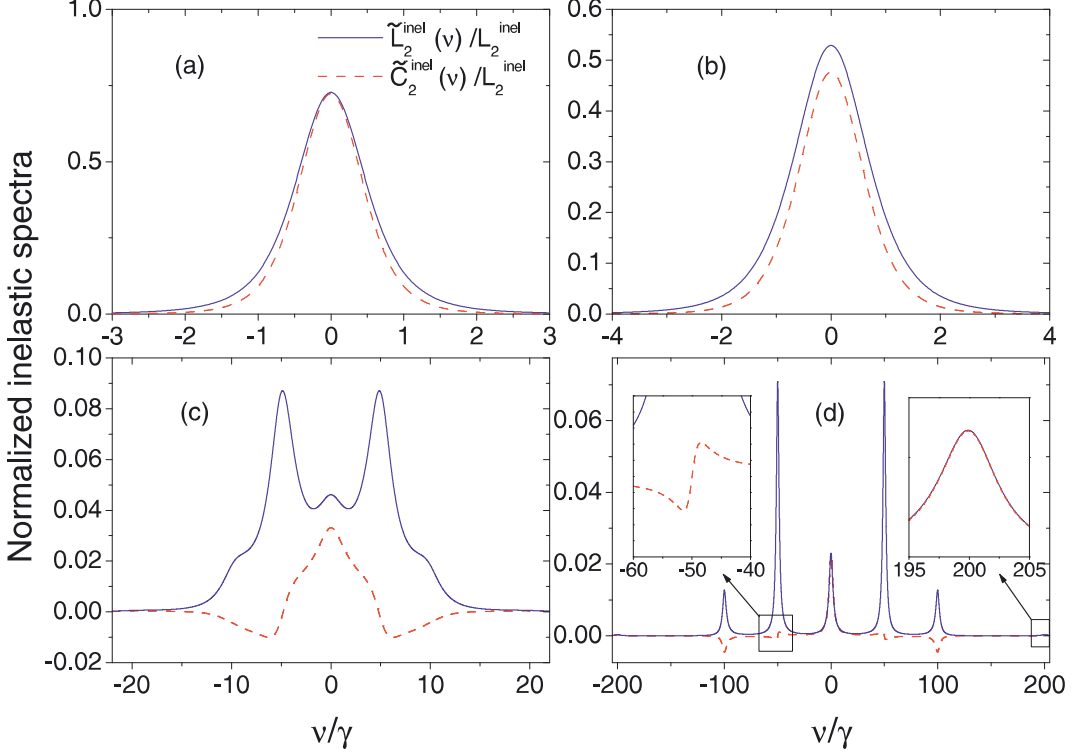


FIG. 3: Normalized inelastic spectra of the ladder (solid line) and crossed (dashed line) terms at exact resonance for different values of the Rabi frequency: (a) $\Omega = 0.1\gamma$; (b) $\Omega = \gamma$; (c) $\Omega = 10\gamma$; (d) $\Omega = 100\gamma$.

the common prefactor $2|\tilde{g}|^2/15$):

$$\tilde{L}_2^{\text{inel}}(\nu) \simeq \frac{1}{\pi} \left(\frac{\Omega}{\gamma} \right)^4 \frac{\gamma^3(2\gamma^2 + \nu^2)}{2(\gamma^2 + \nu^2)^3}, \quad \tilde{C}_2^{\text{inel}}(\nu) \simeq \frac{1}{\pi} \left(\frac{\Omega}{\gamma} \right)^4 \frac{\gamma^5}{(\gamma^2 + \nu^2)^3}. \quad (26)$$

It is easy to establish that the expressions in Eq. (26) are consistent with the behavior of the enhancement factor in the two-photon scattering regime. Integrating $\tilde{L}_2^{\text{inel}}(\nu)$, $\tilde{C}_2^{\text{inel}}(\nu)$ over all frequencies, we obtain the following inelastic ladder and crossed terms for small Ω :

$$L_2^{\text{inel}} \simeq \int_{-\infty}^{\infty} d\nu \tilde{L}_2^{\text{inel}}(\nu) = \frac{7}{16} \left(\frac{\Omega}{\gamma} \right)^4, \quad C_2^{\text{inel}} \simeq \int_{-\infty}^{\infty} d\nu \tilde{C}_2^{\text{inel}}(\nu) = \frac{3}{8} \left(\frac{\Omega}{\gamma} \right)^4. \quad (27)$$

Rewriting Eq. (27) in terms of s and combining it with the small- s expression for the elastic ladder and crossed terms $L_2^{\text{el}} = C_2^{\text{el}} \simeq s$, we recover the linear decrease

$$\alpha = 1 + \frac{s + 3s^2/2}{s + 7s^2/4} \simeq 2 - \frac{s}{4}. \quad (28)$$

As the Rabi frequency Ω increases further on [see Fig. 3(b,c,d)], qualitative differences emerge [on Fig. 3(c,d)] in the behavior of the ladder and crossed terms. First, the spectra

split into several distinct peaks. Second, the crossed term becomes negative for a range of frequencies beyond the central peak. This is a manifestation of destructive self-interference of inelastically scattered photons. Note that a similar effect of *antienhancement* was reported [23] for linear double scattering from atoms with Zeeman-shifted hyperfine ground levels. New spectral features are robust and become well-separated in the asymptotic limit of intense driving [for an example at $\Omega = 100\gamma$, see Fig. 3(d)]. We will next address the approximate analytic expression for CBS spectrum at $\Omega \gg \gamma$, derived in the leading order $\sim (\gamma/\Omega)^2$.

In this case, the explicit expressions for the ladder and crossed spectra can be represented by using a function of two real variables x_1 and x_2 :

$$\mathcal{L}(x_1, x_2) = \frac{1}{\pi} \frac{x_1}{x_1^2 + x_2^2}. \quad (29)$$

Let us mention the properties of $\mathcal{L}(x_1, x_2)$ that are important to us: (i) if $x_1 = \text{Const}$, then function (29) represents a Lorenzian with width x_1 and a resonance at $x_2 = 0$; (ii) if $x_2 = \text{Const}$, then (29) describes a resonance of the dispersive type at $x_1 = 0$.

With the help of the function (29), the ladder and crossed spectra are given by

$$\begin{aligned} \tilde{L}_2^{\text{inel}}(\nu) \simeq & \left(\frac{\gamma}{\Omega}\right)^2 \left(\frac{1}{2} \mathcal{L}(\gamma, \nu) + \frac{1}{4} \mathcal{L}(3\gamma, \nu) + \frac{1}{72} [\mathcal{L}(3\gamma, \nu - 2\Omega) + \mathcal{L}(3\gamma, \nu + 2\Omega)] \right. \\ & + \frac{1}{9} [\mathcal{L}(3\gamma/2, \nu - \Omega) + \mathcal{L}(3\gamma/2, \nu + \Omega)] \\ & + \frac{5}{18} [\mathcal{L}(5\gamma/2, \nu - \Omega) + \mathcal{L}(5\gamma/2, \nu + \Omega)] \\ & \left. + \frac{14}{9} [\mathcal{L}(3\gamma/2, \nu - \Omega/2) + \mathcal{L}(3\gamma/2, \nu + \Omega/2)] \right), \end{aligned} \quad (30)$$

$$\begin{aligned} \tilde{C}_2^{\text{inel}}(\nu) \simeq & \left(\frac{\gamma}{\Omega}\right)^2 \left(\frac{1}{2} \mathcal{L}(2\gamma, \nu) + \frac{1}{4} \mathcal{L}(3\gamma, \nu) - \frac{1}{6} [\mathcal{L}(5\gamma/2, \nu - \Omega) + \mathcal{L}(5\gamma/2, \nu + \Omega)] \right. \\ & + \frac{1}{72} [\mathcal{L}(3\gamma, \nu - 2\Omega) + \mathcal{L}(3\gamma, \nu + 2\Omega)] \left. \right) \\ & + \left(\frac{\gamma}{\Omega}\right)^3 \frac{208}{45} [\mathcal{L}(\nu + \Omega/2, 3\gamma/2) - \mathcal{L}(\nu - \Omega/2, 3\gamma/2)], \end{aligned} \quad (31)$$

where the two terms of order $(\gamma/\Omega)^3$ are retained because they define dispersive resonances of $\tilde{C}_2^{\text{inel}}(\nu)$ at $\nu = \pm\Omega/2$. As seen from Eqs. (30) and (31) as well as from Fig. 3(d), both the ladder and crossed terms have 7 resonances, the resonances of both the ladder and crossed terms at $\nu = 0$ and of the ladder term at $\nu = \pm\Omega$ being sums of two Lorenzians with different widths and weights > 0 . The rest resonances of the ladder term are also Lorenzians with positive weights. Two resonances of the crossed term at $\nu = \pm\Omega/2$ have the dispersive line

shape and, therefore, have no net contribution to the integrated intensity. Furthermore, among the rest five resonances of the crossed term which all are of the Lorenzian type, two at $\nu = \pm\Omega$ have negative weights. Thus, inelastic photons (self-)interfere destructively at $\nu = \pm\Omega$, yet the overall effect of all inelastic processes is constructive. Note also that in the frequency domains where interference is constructive, it is also perfect, as can be concluded from the equality between the respective weights of the ladder and crossed terms.

By performing the elementary integrations of Eqs. (30) and (31), we arrive at the inelastic ladder and crossed terms

$$L_2^{\text{inel}} \simeq \frac{14}{3} \left(\frac{\gamma}{\Omega} \right)^2, \quad C_2^{\text{inel}} \simeq \frac{4}{9} \left(\frac{\gamma}{\Omega} \right)^2, \quad (32)$$

which are consistent with Eqs. (23), (24) and, hence, with $\alpha = \alpha_\infty = 23/21$.

Let us now address the interpretation of the CBS spectrum in the limit of intense driving.

C. Interpretation

One can understand the structure of the CBS spectrum from the analysis of CBS as a specific realization of the pump-probe experiment [a similar view is held by the authors of Ref. [19]]. In the usual setting of such an experiment [24], an atomic transition is simultaneously subjected to two monochromatic fields: a variable-intensity, fixed-frequency driving, or pump, field, and a weak probe field with tunable frequency. For different frequencies of the probe field it can be absorbed or amplified depending on the intensity of the pump field. This occurs because the pump field leads to the energy levels' shifts and broadenings, while the weak field transmission spectrum probes these new resonances; hence the name of this technique.

In our case of CBS with two atoms, an intense pump acts in the $|1\rangle \leftrightarrow |4\rangle$ transitions of both atoms, causing an AC Stark shift of the energy levels. In this case it is instructive to treat the laser mode as a quantum system strongly coupled to the laser-driven atomic transition [25]. The eigenstates of the laser-atom interaction Hamiltonian for $\delta = 0$ are the dressed states

$$|\pm(N)\rangle_\alpha = (|1, N+1\rangle_\alpha \pm e^{i\mathbf{k}\cdot\mathbf{r}_\alpha} |4, N\rangle_\alpha) / \sqrt{2}, \quad (33)$$

where N and $N+1$ refer to the number of photons in the laser mode, and α labels the atoms. Spontaneous transitions from the dressed states manifold $\{|\pm(N)\rangle_\alpha\}$ to $\{|\pm(N-1)\rangle_\alpha\}$

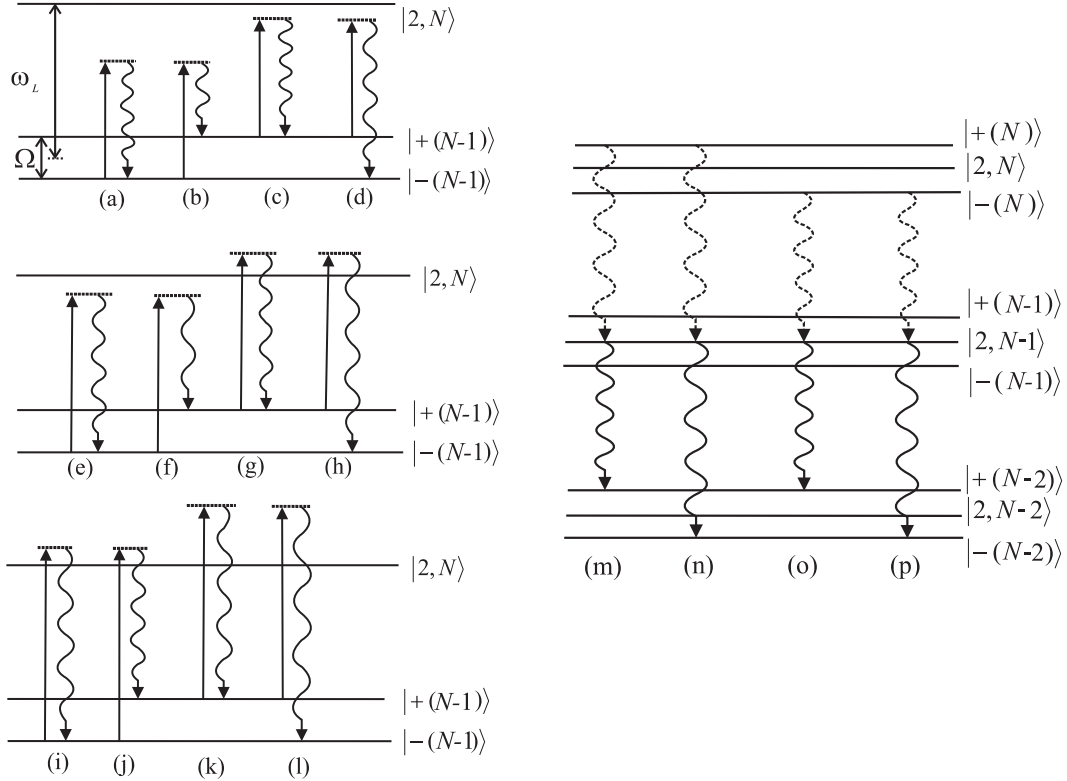


FIG. 4: Scattering processes (a)-(l) and radiative transitions (m)-(p), depicted by solid wavy arrows, contributing to CBS spectra in the regime of intense driving. Horizontal lines indicate dressed states. In the processes (a)-(l), a photon with either of the frequencies emitted by one atom ($\omega_L - \Omega$ (a-d); ω_L (e-h); $\omega_L + \Omega$ (i-l)) undergoes the Rayleigh or Raman scattering on the dressed states $|\pm (N-1)\rangle$. Diagrams (m-n) show radiative cascades in which CBS resonances at $\omega_L \pm \Omega/2$ appear. Level $|2, N\rangle$ can be populated as a result of a multiphoton scattering process with the participation of one doubly scattered photon (depicted by dashed wavy arrows).

lead to emission of the fluorescence spectrum with three symmetric peaks centered at the frequencies $\omega_L - \Omega$, ω_L , and $\omega_L + \Omega$ known as the Mollow triplet [26]. The Mollow triplet emitted by one atom plays a role of the probe for another atom.

Figure 4 illustrates the processes that contribute to the CBS spectrum in $h \parallel h$ channel. The left part Fig. 4(a-l) shows possible one-photon elastic Rayleigh and inelastic Raman processes which photons of frequencies $\omega_L - \Omega$ (a-d), ω_L (e-h), and $\omega_L + \Omega$ (i-l) undergo on the dressed states $|\pm (N-1)\rangle$. The right part of Fig. 4(m-n) shows radiative cascades in the dressed state basis leading to resonances in the CBS spectrum at $\omega_L \pm \Omega/2$. These lines appear as a result of the spontaneous transitions from the state $|2, N-1\rangle$ (note that the

atomic state $|2\rangle$ is not affected by the laser field) to states $|\pm(N-2)\rangle$. This is the notable Autler-Townes doublet [25, 27, 28] emitted from the transition between pairs of states of which only one is a member of the laser-driven transition.

One observes that in all the processes except (b) and (l), several transitions participate in the creation of a CBS photon. Phases between the participating transitions can be opposite due to difference, e.g., in the initial, intermediate, or final atomic states, leading to the negative signs of the interferential contributions around $\omega_L \pm \Omega$ and $\omega_L \pm \Omega/2$.

IV. CONCLUSION

Using the master equation approach we have analytically calculated a spectrum of CBS by two identical, motionless atoms for the case of exact resonance between the laser and atomic transition frequencies. This enabled us to analyse in more detail the previously established [17, 18] effect of the constructive self-interference of inelastically scattered photons.

One conclusion of this analysis is following. The enhancement factor based on the total backscattered light intensity is a poor measure of phase coherence between the counter-propagating waves in the saturation regime, because it has the important information on the character of interference at a given frequency integrated out. At intense driving, one should rather use spectrally resolved measurements with a filter whose passband Γ_f satisfies $\gamma \ll \Gamma_f \ll \Omega$. Then, tuning the filter on individual peaks of the CBS spectra, one would observe either perfect enhancement (at $\omega = \omega_L; \omega_L \pm 2\Omega$), or antienhancement (at $\omega = \omega_L \pm \Omega$), else no net interference at all (at $\omega = \omega_L \pm \Omega/2$).

Another conclusion is that spectral features of CBS can be qualitatively understood from analysis of CBS as a kind of the pump-probe experiment. In the limit of an intense driving, when the spectral line-shape looks rather complicated [see Fig. 4], the ‘pump-probe’ interpretation in combination with the dressed states approach allowed us to identify the origin of all the resonances of the CBS spectrum. Although a detailed explanation of the character of interference between the different processes, in which photons from the probe field (scattered by one atom) are scattered on the dressed states (of another atom), is beyond the scope of this work, the following remark is in order. At exact resonance, some of the processes interfere constructively while some destructively, with the overall effect being constructive. But it is possible to vary populations of the dressed states and, consequently,

the weights of different processes by changing the laser-atom detuning δ . Nothing forbids the overall effect of inelastic photons to be destructive. In fact, we showed in the previous work [18] that for large detuning it is indeed so. We also established in the same paper that the ladder term of double scattering becomes negative in $h \perp h$ channel in the saturation regime. This result can be interpreted as a mere absorption of the probe field.

A challenging problem for the future would be to generalize the results of the present work for moving atoms.

Acknowledgments

I would like to thank Andreas Buchleitner and Cord Müller for the fruitful collaboration and encouragement which made this work possible. Useful discussions with D. Delande, B. Grémaud, S. Ya. Kilin, D. V. Kupriyanov, C. Miniatura, A. P. Nizovtsev, M. O. Scully, I. M. Sokolov, M. Titov, C. Viviescas, and T. Wellens are gratefully acknowledged. Last not least, it is a pleasure to thank the members of the Research Group “Nonlinear Dynamics in Quantum Systems” at the Max Planck Institute for the Physics of Complex Systems for the friendly and creative atmosphere during my visits there.

- [1] H. J. Metcalf and P. van der Straten, *Laser Cooling and Trapping* (Springer, New York, 1999).
- [2] M. H. Anderson *et al.*, Science **269**, 198 (1995). C. C. Bradley *et al.*, Phys. Rev. Lett. **75**, 1687 (1995). K. B. Davis *et al.*, Phys. Rev. Lett. **75**, 3969 (1995).
- [3] E. Akkermans, G. Montambaux, J.-L. Pichard, and J. Zinn-Justin (Eds.) *Mesoscopic Quantum Physics* (Elsevier, Amsterdam, 1994).
- [4] G. Labeyrie, F. de Tomasi, J.-C. Bernard, C. A. Müller, C. Miniatura and R. Kaiser, Phys. Rev. Lett. **83**, 5266 (1999).
- [5] P. Kulatunga, C. I. Sukenik, S. Balik, M. D. Havey, D. V. Kupriyanov, and I. M. Sokolov, Phys. Rev. A **68**, 033816 (2003).
- [6] D. V. Kupriyanov, I. M. Sokolov, C. I. Sukenik, and M. D. Havey, Laser Phys. Lett. **3**, 223 (2006).
- [7] C. A. Müller, T. Jonckheere, C. Miniatura, and D. Delande, Phys. Rev. A **64**, 053804 (2001).

- [8] C. A. Müller and C. Miniatura, *J. Phys. A* **35**, 10163 (2002).
- [9] D. V. Kupriyanov, I. M. Sokolov, P. Kulatunga, C. I. Sukenik, and M. D. Havey, *Phys. Rev. A* **67**, 013814 (2003).
- [10] G. Labeyrie, D. Delande, C. A. Müller, C. Miniatura, and R. Kaiser, *Europhys. Lett.* **61**, 327 (2003).
- [11] T. Chanelière, D. Wilkowski, Y. Bidel, R. Kaiser, and C. Miniatura, *Phys. Rev. E* **70**, 036602 (2004).
- [12] T. Wellens, B. Grémaud, D. Delande, and C. Miniatura, *Phys. Rev. A* **70**, 023817 (2004).
- [13] T. Wellens, B. Grémaud, D. Delande, and C. Miniatura, *Phys. Rev. E* **71**, 055603(R) (2005); *Phys. Rev. A* **73**, 013802 (2006).
- [14] A. A. Golubentsev, *Zh. Eksp. Teor. Fiz.* **86**, 47 (1984) [*Sov. Phys. JETP* **59**, 26 (1984)].
- [15] G. Labeyrie, C. A. Müller, D. S. Wiersma, Ch. Miniatura, and R. Kaiser, *J. Opt. B: Quantum Semiclassical Opt.* **2**, 672 (2000).
- [16] D. V. Kupriyanov, I. M. Sokolov, N. V. Larionov, P. Kulatunga, C. I. Sukenik, S. Balik, and M. D. Havey, *Phys. Rev. A* **69**, 013814 (2004).
- [17] V. Shatokhin, C. A. Müller, and A. Buchleitner, *Phys. Rev. Lett.* **94**, 043603 (2005).
- [18] V. Shatokhin, C. A. Müller, and A. Buchleitner, *Phys. Rev. A* **73**, 063813 (2006).
- [19] B. Grémaud, T. Wellens, D. Delande, C. Miniatura, e-print quant-ph/0506010.
- [20] R. J. Glauber, “Optical Coherence and Photon Statistics” in *Quantum Optics and Electronics*, edited by C. DeWitt, A. Blandin, and C. Cohen-Tannoudji (Gordon and Breach, London, 1965).
- [21] M. O. Scully and M. S. Zubairy, *Quantum Optics*, (Cambridge University Press, Cambridge, 1997).
- [22] R. H. Lehmberg, *Phys. Rev. A* **2**, 883 (1970).
- [23] D.V. Kupriyanov, I.M. Sokolov, and M.D. Havey *Opt. Commun.* **243**, 165 (2004).
- [24] B. R. Mollow, *Phys. Rev. A* **5**, 2217 (1972); F. Y. Wu, S. Ezekiel, M. Ducloy, and B. R. Mollow, *Phys. Rev. Lett.* **38**, 1077 (1977).
- [25] C. Cohen-Tannoudji, J. Dupont-Roc, G. Grynberg, *Atom-Photon Interactions* (Wiley, New York, 1992).
- [26] B. R. Mollow, *Phys. Rev.* **188**, 1969 (1969).
- [27] S. H. Autler and C. H. Townes, *Phys. Rev.* **100**, 703 (1955).

[28] B. R. Mollow, Phys. Rev. A **5**, 1522 (1972).